Fluorescence-based methods for measuring target interference by CRISPR-Cas systems

Phong T. Phan¹, Michael Schelling¹, Chaoyou Xue^{1,2} and Dipali G. Sashital^{1*}

¹Roy J. Carver Department of Biochemistry, Biophysics and Molecular Biology, Iowa State University,

Ames, IA 50011, USA

²Present address: Department of Biochemistry and Molecular Biophysics, Columbia University, New

York, NY, USA 10032

Address correspondence to: Dipali Sashital, sashital@iastate.edu

ABSTRACT

Type I, II and V CRISPR-Cas systems are RNA-guided dsDNA targeting defense mechanisms

found in bacteria and archaea. During CRISPR interference, Cas effectors use CRISPR-derived RNAs

(crRNAs) as guides to bind complementary sequences in foreign dsDNA, leading to the cleavage and

destruction of the DNA target. Mutations within the target or in the protospacer adjacent motif (PAM) can

reduce the level of CRISPR interference, although the level of defect is dependent on the type and

position of the mutation, as well as the guide sequence of the crRNA. Given the importance of Cas

effectors in host defense and for biotechnology tools, there has been considerable interest in developing

sensitive methods for detecting Cas effector activity through CRISPR interference. In this chapter, we

describe an in vivo fluorescence-based method for monitoring plasmid interference in Escherichia coli.

This approach uses a green fluorescent protein (GFP) reporter to monitor varying plasmid levels within

bacterial colonies, or to measure the rate of plasmid loss in bacterial populations over time. We

demonstrate the use of this simple plasmid loss assay for both chromosomally integrated and plasmid-

borne CRISPR-Cas systems.

KEYWORDS

CRISPR-Cas; CRISPR interference; Cascade; Cas9; GFP; fluorescence imaging; flow cytometry;

Typhoon imager; molecular biology

1. INTRODUCTION

CRISPR—Cas (clustered regularly interspaced short palindromic repeats-CRISPR associated) systems are RNA-guided immune systems that allow archaea and bacteria to fight off invading nucleic acids (Marraffini, 2015; Sorek, Lawrence, & Wiedenheft, 2013). CRISPR immunity proceeds through three main stages: adaptation, expression and maturation, and interference. During adaptation, the host activates the CRISPR system by inserting a short fragment of foreign DNA into its chromosome as a new spacer following the first repeat of the CRISPR array. The CRISPR array is transcribed and processed into mature CRISPR RNAs (crRNAs), each containing a different spacer sequence. Finally, during CRISPR interference, Cas effector proteins use crRNAs as a guide to bind protospacer sequences that match the crRNA spacer. The target is then destroyed via endonucleolytic activity of a Cas protein.

CRISPR-Cas systems are divided into two main classes, class 1 and class 2 (Koonin, Makarova, & Zhang, 2017; Makarova et al., 2015). The classes are divided into three types each (types I, III and IV for class 1 and types II, V and IV for class 2), each of which is further divided into subtypes (e.g. subtypes I-A to I-F and I-U). Class 1 systems utilize multisubunit crRNA-effector complexes and in some cases requires a separate Cas endonuclease for CRISPR interference. For class 2 systems, a single protein acts as crRNA effector and endonuclease. The mechanisms of CRISPR interference also varies between types. Type I, II and V Cas effectors bind and directly destroy dsDNA targets (Garneau et al., 2010; Gasiunas, Barrangou, Horvath, & Siksnys, 2012; Jinek et al., 2012; Jore et al., 2011; Mulepati & Bailey, 2013; Westra et al., 2012; Zetsche et al., 2015), while type III and VI Cas effectors are activated as non-specific nucleases upon binding to RNA targets (Abudayyeh et al., 2016; Elmore et al., 2016; Estrella, Kuo, & Bailey, 2016; Hale et al., 2009; Kazlauskiene, Tamulaitis, Kostiuk, Venclovas, & Siksnys, 2016). The type I dsDNA-targeting systems are currently believed to be the most abundant CRISPR-Cas systems found in nature (Makarova et al., 2015). While less common in nature, type II and V single-protein Cas effectors have been co-opted as extremely effective biotechnology tools, due to their easily programmable dsDNA binding and cleavage activities (Hsu, Lander, & Zhang, 2014; Murugan,

Babu, Sundaresan, Rajan, & Sashital, 2017). Thus, the mechanism and sequence determinants of dsDNA targeting CRISPR-Cas systems has been of considerable interest to the research community.

During CRISPR interference against dsDNA, the Cas effector complex searches for targets by locating the protospacer adjacent motif (PAM), a short sequence required for target binding and selfversus-non-self-discrimination in type I, II and V CRISPR-Cas immunity (Deveau et al., 2008; Jinek et al., 2012; Mojica, Diez-Villasenor, Garcia-Martinez, & Almendros, 2009; Sashital, Wiedenheft, & Doudna, 2012; Semenova et al., 2011; Zetsche et al., 2015) (Figure 1A). PAM recognition by the Cas effector is thought to destabilize the dsDNA duplex, enabling crRNA strand invasion and base pairing between the crRNA spacer and target strand of the dsDNA (Redding et al., 2015; Sashital et al., 2012; Sternberg, Redding, Jinek, Greene, & Doudna, 2014; Xue, Zhu, Zhang, Shin, & Sashital, 2017). This R-loop forms directionally away from the PAM, and formation of the crRNA-DNA hybrid offsets the thermodynamic penalty of dsDNA unwinding (Rutkauskas et al., 2015; Szczelkun et al., 2014). As a result, the first several PAM-proximal positions of the target are extremely important for binding, forming a "seed" sequence (Semenova et al., 2011; Wiedenheft et al., 2011) (Figure 1A). Mutations within the dsDNA target, especially the PAM and seed sequence, can lead to phage escape or decreased interference against plasmids (Datsenko et al., 2012; Fineran et al., 2014; Semenova et al., 2011; Xue et al., 2015). Conversely, mismatches between crRNA and target outside of the seed have less effect on Cas effector function, and can lead to off-target effects during CRISPR-based genome editing experiments using class 2 effectors (Fu et al., 2013; Hsu et al., 2013; Kim et al., 2016; Kleinstiver, P Benjamin et al., 2016).

Methods for measuring the efficiency of CRISPR interference are required to evaluate the effects of target mutations on CRISPR immunity and the potential for off-target effects during genome editing. In this chapter, we describe a simple and sensitive method for measuring CRISPR interference against dsDNA. Our method relies on a fluorescent readout to detect the level of plasmid interference in *E. coli* cells. Cellular fluorescence can be determined using fluorescence imaging of colonies or of individual cells, allowing for rapid qualitative or quantitative measurement of the relative efficiency of plasmid

degradation. We demonstrate the effectiveness of this plasmid loss assay using multiple measurement techniques and CRISPR-Cas systems and provide detailed procedures for these methods.

2. FLUORESCENCE-BASED STRATEGIES FOR MEASURING CRISPR INTERFERENCE

Several studies have monitored plasmid loss to determine the effectiveness of CRISPR interference using E. coli as a model organism (Cooper, Stringer, & Wade, 2018; Fineran et al., 2014; Sapranauskas et al., 2011; van Erp et al., 2015; Westra et al., 2013; Xue et al., 2015; Xue, Whitis, & Sashital, 2016). In these experiments, cells are transformed with a plasmid containing a target sequence matching a crRNA expressed within the cell. Degradation of the target plasmid upon uptake can be monitored by measuring the colony forming units (CFU) on antibiotic-containing plates following transformation. At high levels of CRISPR interference, the target plasmid is degraded sufficiently to inhibit colony formation due to the lack of antibiotic resistance gene expression from the plasmid, reducing the transformation efficiency (Cooper et al., 2018; Sapranauskas et al., 2011; Westra et al., 2013). However, this method is not ideal for measuring degradation of target plasmids with intermediate or low levels of CRISPR interference, especially targets with mutations in the PAM or seed. Although target plasmid concentration may be decreased, sufficient antibiotic resistance gene expression can still occur, which could result in slower colony growth but not in a substantial decrease in CFU. Intermediate levels of CRISPR interference can be measured by growing colonies containing target plasmids in nonselective liquid media cultures, plating on non-selective plates, and then replica plating individual colonies onto antibiotic-containing plates (Fineran et al., 2014; Xue et al., 2015). While growth in liquid cultures provides additional time for plasmid degradation, this technique is low throughput and still does not allow for detection of intermediate plasmid concentrations in cells.

As an alternative to antibiotic sensitivity, we previously developed a green fluorescent protein (GFP) reporter assay for measuring CRISPR interference (Xue et al., 2015). In this reporter system, the CRISPR target plasmid contains a constitutively expressed *gfp* gene (Figure 1B-C). Cells transformed with the plasmid are fluorescent, but fluorescence decreases upon plasmid degradation through CRISPR

interference (Figure 1D). The fluorescent readout theoretically enables detection of intermediate levels of target plasmid within colonies or individual cells. Cells in which plasmid copy number has decreased to an intermediate level display intermediate levels of fluorescence as measured by fluorescence imaging or flow cytometry (Xue et al., 2016). Alternatively, cell cultures can be separated into GFP negative (GFP-) and positive (GFP+) populations (i.e. CRISPR interference active and inactive, respectively) using fluorescence activated cell sorting (FACS) (Xue et al., 2015). In this section, we describe the development and validation of this GFP-reporter assay for CRISPR interference.

2.1 Design and development of GFP-reporter plasmid pACYC-GFP

Several important considerations must be accounted for when designing a GFP-expression-based plasmid-loss assay. The reporter plasmid must be stable in the absence of antibiotic selection to ensure that plasmid loss only occurs through CRISPR interference. Cells with and without the plasmid must have identical growth rates to ensure that cultures with mixed populations do not become artificially dominated by one subpopulation. The cells must be sufficiently fluorescent to distinguish between GFP+ and GFP-populations. It is also important to tightly link the presence of the GFP to the presence of the plasmid. This requires not only that the reporter constitutively express GFP, but also that fluorescence must decrease to background in the absence of the plasmid.

We previously reported the pACYC-GFP reporter plasmid (Xue et al., 2015), which was developed to meet the requirements described above (Figure 1B). We cloned *gfp* between BgIII and XhoI restriction sites in the second multiple cloning site (MCS) of pACYCDuet-1, leaving the first MCS (MCS1) free for insertion of CRISPR targets (Figure 1A-B). We initially added a *tac* promoter upstream of the *gfp* gene for constitutive expression (Figure 1C, 2A). However, we determined in initial experiments that cells carrying this plasmid grew more slowly than cells that had lost the plasmid following CRISPR interference, causing GFP- cells to rapidly overtake the population. This slow growth was likely due to the use of the relatively strong *tac* promoter and the subsequent burden placed on the cells due to GFP overexpression. To reduce the promoter strength, we replaced the native tac promoter

with four tac-derived promoters (promoters 1-4) with variations in the length of sequence between -35 and -10 sites (promoter 1) or in the -35 site sequence (promoters 2-4) (De Mey, Maertens, Lequeux, Soetaert, & Vandamme, 2007) (Figure 2A-B). Of these promoters, promoters 3 and 4 had no effect on the doubling time of *E. coli*, and promoter 3 maintained a sufficient level of fluorescence for easily distinguishing between GFP+ and GFP- populations by flow cytometry (Figure 2B).

To link the presence of GFP to the presence of the plasmid, we added degradation tags to the C-terminus of GFP to reduce the half-life of the protein product (Figure 1C). We tested the *ssrA* peptide-tag AANDENYALAA and two additional sequences in which the last three residues of the tag were changed to AAV or ASV, which has previously been shown to reduce the rate of degradation (Andersen et al., 1998). For the promoter 3 construct, only the ASV variant produced sufficient fluorescence for measurement in cells. This plasmid containing *gfp* under control of promoter 3 and containing the ASV *ssrA* tag is hereafter referred to as pACYC-GFP (Figure 1B-C). Importantly, competition assays between *E. coli* cells bearing either empty pACYCDuet-1 or pACYC-GFP indicated that GFP expression does not affect the ratio of GFP- and GFP+ cells, as ratios between the two strains remained constant after 24 h growth (with sub-culturing at 12 h) without antibiotic selection (Figure 2C). This experiment demonstrates that pACYC-GFP is stable and does not alter the growth rate of *E. coli* cells.

For the experiments described in section 3, we also created a variant of the plasmid containing an ampicillin resistance marker. These experiments were performed in *E. coli* K12 BW40114, which contains a chloramphenical acetyltransferase (*cat*) gene within the *cas* operon (Datsenko et al., 2012) and would not be compatible with the CmR version of pACYC-GFP. The ampicillin marker was amplified from pFastBac vector and ligated to pACYC-GFP between ScaI and BsaAI sites (Figure 1B). The remaining backbone, including origin of replication, MCS1 and GFP-expression cassette, are unchanged.

2.2 Validation of GFP-based plasmid-loss assay

We have previously validated the GFP reporter plasmid loss assay using the type I-E CRISPR-Cas system present in *E. coli* K12 (Xue et al., 2015, 2016). In this system, CRISPR interference is carried out by the crRNA-effector complex Cascade, which is required for target binding, and the endonuclease

Cas3, which is required for target destruction (Brouns et al., 2008; Mulepati & Bailey, 2013; Westra et al., 2012). In *E. coli* K12, H-NS (heat-stable nucleoid-structuring protein) has been shown to be a transcriptional repressor of the type I-E *cas* operon (Medina-Aparicio et al., 2011; Pougach et al., 2010; Pul et al., 2010; Swarts et al., 2014; Westra et al., 2010). Deletion of *hns* partially relieves this repression, which results in constitutive activation of the CRISPR-Cas system (Pougach et al., 2010; Westra et al., 2010). We have previously demonstrated the use of pACYC-GFP plasmid loss assays in *E. coli* K12 *hns*-strains (Xue et al., 2015, 2016). Our previous experiments show that the plasmid is stable in the absence of a CRISPR target or in strains in which the *csel* gene is deleted. This gene encodes the large subunit of Cascade that is required for target binding and Cas3 recruitment (Hochstrasser et al., 2014; Sashital et al., 2012). When a CRISPR target is added to pACYC-GFP and the plasmid is transformed to a strain containing an intact CRISPR-Cas system, the plasmid is rapidly degraded and GFP fluorescence decreases in cells, as monitored by flow cytometry (Xue et al., 2015).

In a prior study, we used pACYC-GFP as the backbone for target libraries in which the PAM or seed region of the target were randomized (Xue et al., 2015). This study demonstrated the utility of the GFP reporter system to rapidly assess the overall effects of target mutations on CRISPR-Cas activity. We have also used the plasmid-loss assay as a sensitive method to detect low levels or absence of CRISPR interference upon individual PAM or seed mutations (Xue et al., 2016). By using flow cytometry, we were able to detect cell populations with intermediate fluorescence levels upon mutation of the first position of the seed or the AAG PAM to AAA, revealing that these mutations cause defects but do not completely ablate CRISPR interference. In contrast, mutation of the PAM to AGA yielded fluorescence levels that were unchanged from the empty pACYC-GFP plasmid lacking a CRISPR target, demonstrating that this PAM mutation completely blocks CRISPR interference in the *E. coli* K12 *hns*-strain.

In our previous studies, we monitored CRISPR interference in liquid cultures using flow cytometry at a set time point. However, plasmid loss can be measured using alternative methods, such as fluorescence imaging, or over a time course to monitor the efficiency of CRISPR interference. In the next

two sections, we describe multiple methods for using the pACYC-GFP reporter system to study CRISPR interference, expanding the utility of the fluorescence-based plasmid-loss assay.

3. MEASUREMENT OF CRISPR INTERFERENCE IN COLONIES AND LIQUID CULTURE

We have previously shown that some PAM and seed mutations cause more severe defects than others. In particular, for the first crRNA expressed from CRISPR 2 within the *E. coli* K12 genome (spacer 2.1), we have shown that mutation of the AAG PAM to AAA or AGA causes intermediate or very low levels of interference, respectively (Xue et al., 2015, 2016). Similarly, mutations at positions 1 or 4 of the seed sequence cause varying levels of defects. While a G1C mutation is tolerated, an A4G mutation causes a severe decrease in interference (Xue et al., 2015). Using these mutant targets in comparison with a perfect target, we demonstrate here the utility of pACYC-GFP-based plasmid loss assays for detecting varying levels of CRISPR interference in colonies and liquid cultures. First, we describe how CRISPR targets can be added to pACYC-GFP using a simple oligonucleotide-based cloning technique. Next, we describe the use of a Typhoon scanner to image fluorescence intensity of *E. coli* colonies that have undergone varying degrees of CRISPR interference based on variations in their target sequences. Finally, we describe an extension our previous experimental protocol for measuring CRISPR interference in liquid cultures using flow cytometry to monitor plasmid loss over time.

3.1 Addition of CRISPR target to pACYC-GFP

For CRISPR interference assays, a target must be added to pACYC-GFP. We left MCS1 intact within pACYC-GFP, enabling insertion of oligonucleotides bearing CRISPR targets between restriction sites. CRISPR targets were designed as complementary oligonucleotides containing PAM and protospacer flanked on either side by overhanging sequences matching restriction enzyme products (Figure 3A). For experiments described in sections 3.2 and 3.3, we designed targets for spacer 2.1 in the *E. coli* genome. We introduced spacer 2.1 targets with a perfect PAM and protospacer sequence, or with G1C, A4G, AAA PAM or AGA PAM mutations. Similar methods can be used to insert target sequences for crRNA sequences introduced exogenously, as described in section 4.

3.1.1 Equipment

- Heat block for 37°C and 95°C incubations
- Agarose gel apparatus

3.1.2 Buffers and reagents

- T4 polynucleotide kinase (PNK), NotI, NcoI, T4 DNA ligase and accompanying buffers purchased from New England Biolabs
- 100 mM ATP
- 100 μM CRISPR target oligonucleotides (designed as in Figure 3A) and pACYC-GFP
- Gel purification kit (e.g. Qiagen QIAquick Gel Extraction kit or Promega Wizard SV Gel and PCR Clean-Up System)
- One Shot TOP10 Competent Cells (Thermo-Fisher) or similar cloning E. coli strain
- Miniprep kit (Qiagen or Promega)

3.1.3 Procedure

- Phosphorylate the 5'-end of each oligonucleotide by adding 1 μL oligonucleotide (10 μM final), 1 μL 10X T4 PNK Buffer (1X final), 1 μL ATP (10 mM final), 0.5 μL T4 PNK and 6.5 μL ddH₂O.
 Incubate 30 min at 37°C. Heat inactivate the PNK by incubating the reaction at 65°C for 15 min.
- 2. Anneal oligos by mixing 5 μ L of each phosphorylation reaction, incubating 5 min at 95 °C, and cooling at room temperature for 10 min.
- Digest 1.5 μg pACYC-GFP with 2 μL each of NotI and NcoI in 1X CutSmart Buffer in 50 μL total reaction volume. Incubate overnight at 37°C, then purify digested vector on 1% agarose gel using directions provided by gel purification kit.
- 4. For ligation, add 1 μ L of annealed oligonucleotides, 60 ng of digested pACYC-GFP vector, 1 μ L 10X T4 DNA ligase buffer, and 0.5 μ L of T4 DNA ligase in a total volume of 10 μ L. Incubate overnight at 16°C.

5. Transform 5 μL of ligation reaction into 100 μL aliquot of competent cells using standard methods. Plate cells on LB media supplemented with the appropriate antibiotic. Negative control ligations (no oligonucleotides added) can be run in parallel to determine the amount of background colonies. We generally prepare plasmids from 3 colonies using standard miniprep kits (e.g. Qiagen or Promega). Ensure correct sequence insertion by Sanger sequencing using DuetUp1 primer (5'-GGATCTCGACGCTCTCCCT-3').

3.2 Detection of plasmid levels in bacterial colonies

In this section we describe the use of fluorescence imaging to visualize the efficiency of CRISPR interference in *E. coli* K12 colonies following transformation of pACYC-GFP containing a CRISPR target. Typhoon fluorescence imaging has been shown to be more sensitive, robust and high throughput compared to other fluorescence microscopies for detection of GFP-expressing cells (Hilly & Liu, 2009). The Typhoon imager is able to detect varying levels of GFP-based fluorescence, indicating the varying levels of plasmid present in colonies. Here, we describe measurement of CRISPR interference in *E. coli* K12 BW40114 colonies, a strain that was previously developed in the laboratory of Konstantin Severinov (Datsenko et al., 2012). In this strain, the *cas3* and *cse1* (controlling expression of all Cascade genes) promoters are replaced with *lacUV5* and *araBp8*, respectively, which are induced by isopropyl β-D-1-thiogalactopyranoside (IPTG) and arabinose, respectively. For the assays described in this section, the *cas* promoters were induced upon plating cells transformed with pACYC-GFP target plasmids due to the presence of both inducers in the LB plates. Induction at this stage allowed for measurement of varying levels of CRISPR interference for the five targets tested.

The ability to detect variations in CRISPR interference within colonies is demonstrated by comparing the perfect spacer 2.1 target with the four mutant targets (Figure 3B-C). Following Typhoon imaging of the plates, the varying levels of fluorescence intensity can be observed qualitatively (Figure 3B). Consistent with our previous results, the G1C causes only a slight defect in CRISPR interference, as observed by the slightly greater intensity of colonies in comparison to the perfect target. The AAA PAM

displays intermediate levels of interference, while the A4G and AGA PAM mutations are the most severe, with intensities comparable to colonies harboring empty pACYC-GFP that lacked a CRISPR target.

In addition to qualitative assessment of relative Cascade/Cas3 activity, we also quantified the intensity of individual colonies to measure the fluorescence of bacteria harboring each target plasmid (Figure 3C). Quantitation was performed using freely-available open-source image processing software. Using this method, hundreds of data points can be obtained from a single plate, allowing graphical depictions that account for the distribution of fluorescence across all colonies. We plotted normalized intensities using a box plot (Figure 3C), revealing the varying levels of fluorescence intensity based on the level of CRISPR interference. This method of data visualization reveals that fluorescence intensity is more variable for the two pACYC-GFP targets, A4G and AGA PAM, that undergo very low levels of CRISPR interference, although the variability is similar to that observed for the empty pACYC-GFP plasmid. The following sub-sections describe the exact methods used for qualitative and quantitative assessment of fluorescence levels in pACYC-GFP-bearing colonies.

3.2.1 Equipment

- Microcentrifuge and centrifuge for 15 mL culture tubes (4°C)
- Incubators (37°C, for plates and shaking) and water bath (42°C)
- Spectrophotometer
- Typhoon FLA 9500 (GE Healthcare) with ImageQuant TL software
- ImageJ software with Colony Counter plugin installed following directions at https://imagej.nih.gov/ij/plugins/colony-counter.html

3.2.2 Buffers and Reagents

- LB plates (1.5% agar) containing chloramphenicol (34 μg/mL)
- LB plates (1.5% agar) containing ampicillin (100 μg/mL), IPTG (1 mM) and arabinose (1 mM)
- LB media
- Chloramphenicol dissolved in 95% ethanol (34 mg/mL)

- Buffer 1: 80 mM MgCl₂, 20 mM CaCl₂, autoclaved and stored at 4°C
- Buffer 2: 100 mM CaCl₂, 16% Glycerol, pH adjusted to 7, autoclaved and stored at 4°C

3.2.3 Procedure

- 1. Streak BW40114 strain from a glycerol stock onto an LB plate containing chloramphenicol and incubate overnight at 37°C. Note that the two non-native promoters in BW40114 are separated by a chloramphenicol acetyltransferase (*cat*) gene, which can be used as a selection marker for the strain. Due to the presence of the chromosomal *cat* gene, we used pACYC-GFP constructs containing an ampicillin resistance marker (Figure 1B) for the plasmid loss assays.
- 2. Grow a single colony from the streak plate in 2 mL LB media supplemented with 2 μL chloramphenicol in a 15 mL culture tube (VWR) at 37°C with shaking at 180 rpm overnight.
- 3. Inoculate 2 mL LB supplemented with 2 μL chloramphenicol (34 μg/mL final) with 20 μL of the overnight culture in a 15 mL culture tube. Each 2 mL culture will yield enough competent cells for four transformations, so multiple cultures can be grown if additional transformations will be performed. Grow at 37°C for 2 h with shaking at 180 rpm. Measure the optical density at 600 nm (OD600) for 1 mL of the culture using a spectrophotometer, leaving 1 mL of culture for preparation of competent cells. The OD600 should be between 0.3-0.4 after 2 h growth.
- Chill the culture tube on ice for 10 minutes and then centrifuge at 4000 × g for 5 min at 4°C.
 Carefully remove the supernatant from the cell culture and resuspend in 800 μL chilled Buffer 1.
- 5. Centrifuge at 4000 × g for 5 min at 4°C. Carefully remove the supernatant and resuspend the cell pellet in 130 μL of pre-chilled Buffer 2.
- Chill the competent cells on ice for 10 min. Aliquot 30 μL of cells into four pre-chilled 1.5 ml microcentrifuge tube for plasmid transformation.
- 7. To transform the cells, add 100 ng of plasmid DNA to the competent cells and gently flick tubes to mix. Incubate on ice for 30 min. Heat shock cells at 42°C for 30 s in a water bath. Place cells on ice for 5 min. For recovery, add 970 mL LB and incubate at 37°C with shaking at 180 rpm for 1 h.

- 8. Dilute 10 μL of each recovery culture with 90 μL LB. For each transformation, plate the 100 μL of diluted cells onto a pre-warmed LB plate containing 100 μg/mL ampicillin, 1 mM IPTG and 1 mM arabinose. Incubate the plates overnight (16-18 h) at 37°C.
- 9. To detect GFP fluorescence of colonies, scan the plates using a Typhoon FLA 9500 (GE Healthcare). On the Typhoon software, set the excitation wavelength and photo-multiplier tube (PMT) to 473 nm laser-powered blue light and 300 V, respectively. Select the emission filter for scanning green fluorescence emitted from GFP. Set the pixel size to 100 μm with normal sensitivity. Export the scanned image in TIFF format using ImageQuant TL software.
- 10. To measure the fluorescence intensity, open the TIFF image in ImageJ (Rueden et al., 2017; Schneider, Rasband, & Eliceiri, 2012) with the Colony Counter plugin installed (https://imagej.nih.gov/ij/plugins/colony-counter.html). Using the circle select tool, select individual colonies and add them using the "Add" function on the Colony Counter menu. When all colonies are selected, measure the intensity using the "Measure" function on the Colony Counter menu. We recommend measuring colonies from one plate at a time to help keep track of which colonies belong to which plate. The mean intensities of the colonies from each plate can be plotted as a box plot using standard graphing software to show the variations in levels of CRISPR interference for each type of target. For Figure 3C, we normalized mean intensities for individual colonies against the average mean intensity of the empty pACYC-GFP colonies ([mean intensity for colony]/[average mean intensity for all empty pACYC-GFP colonies]).

3.3 Measurement of CRISPR interference efficiency in liquid cultures

One of the benefits of the GFP reporter assay is the ability to measure the progress of CRISPR interference over time. By using an inducible strain, cultures bearing different target plasmids can be synchronized to initiate CRISPR interference upon induction of the *cas* promoters. The efficiency of plasmid loss can be measured at different time points by measuring the GFP- cell population using flow cytometry. For the five CRISPR targets used above, we measured plasmid loss over time using this

strategy (Figure 4). Time points were taken following induction, and the average percentage of GFP- cells from multiple cultures were plotted versus time. The resulting curves illustrate the relative efficiencies of the four mutant targets. As we have shown previously, the G1C mutation of spacer 2.1 is far less deleterious than A4G, while the AAA PAM mutation is more tolerated for CRISPR interference than AGA (Xue et al., 2015). By monitoring CRISPR interference at multiple time points, we observe that the G1C mutation does cause a slight defect in comparison to the perfect target, although eventually the G1C target plasmid is lost to a similar degree. These data demonstrate the importance of measuring CRISPR interference over time, and the usefulness of the GFP reporter assay for this purpose. In the following subsections, we describe this simple assay, including methods for measuring pACYC-GFP levels using flow cytometry.

3.3.1 Equipment

- Shaking incubator (37°C)
- Spectrophotometer
- BD Biosciences FACSCanto (San Jose, CA)

3.3.2 Buffers and Reagents

- LB media
- Ampicillin (100 mg/mL)
- IPTG (1M) and arabinose (1M)
- 10X Phosphate Buffered Saline (PBS): 80 g NaCl, 2 g KCl, 25.6 g Na₂HPO₄, 2 g KH₂PO₄
 dissolved in 1 L ddH₂O, pH adjusted to 7.2, filtered with 0.2 μm Millipore Nylon Membrane filter and stored at room temperature

3.3.3 Procedure

 Perform transformation of CRISPR target plasmids in BW40114 as described above, plating on LB plates containing ampicillin without inducers. For starter cultures, inoculate individual colonies from each plate in 2 mL LB supplemented with 2 μL ampicillin (100 μg/mL final) in a

- 15 mL culture tube at 37°C with shaking at 180 rpm. Grow ~ 2 h until the cells reach OD600 of ~0.3. The exact OD600 can be measured for 1 mL of the culture using a spectrophotometer. For each CRISPR target, cultures can be started from multiple colonies to provide biological replicates. We performed measurements for starter cultures from 2-4 individual colonies for each target plasmid.
- Sub-culture 2 μL of each starter culture into pre-warmed 2 mL LB supplemented with 2 μL IPTG (1 mM final) and 20 μL arabinose (10 mM final) in a 15 mL culture tube. Store the rest of the starter culture at 4°C for measurement as the first time point (0 h).
- 3. Grow the culture at 37°C with shaking at 180 rpm. Collect 50 μL at one-hour intervals between 4 h to 10 h post-induction and store overnight at 4°C. We have found that overnight storage at 4°C does not affect the GFP+/GFP- populations in samples.
- 4. For each sample, add 995 μ L of 1X PBS to a clear polystyrene plastic culture tube (Fisher). Add 5 μ L of cells to the tube.
- 5. For flow cytometry analysis, set the excitation wavelength for GFP at 488 nm and the emission wavelength at 525/50 (500 nm to 550 nm) through the fluorescein isothiocyanate (FITC) filter.
 Apply the samples via the sample injection port.
- 6. Create a forward side scattering (FSC) versus side scatter (SSC) dot plot using BDFACSDiva v 8.0.1 software. Set the FSC/SSC dot plot to exclude small particles, debris or dead cells. We set a gate between 10¹ and 10² arbitrary units for both FSC and SSC. For *E. coli* cells, set all the voltages for the flow cytometer's photomultiplier tubes (PMTs) in log scale as the following: FSC at 429 V, SSC at 424 V and FL1 at 480 V. Set threshold of SSC at 200 V.
- 7. Continue measurements until the desired number of events has been reached inside or outside the gate. For data plotted in Figure 4, 10,000 live cells were gated. The average percentage of GFP-cells can be plotted versus time using standard graphing software, as shown in Figure 4.

4. MEASURING CRISPR INTERFERENCE FROM A PLAMID-BORNE CAS EFFECTOR

In addition to assessing activity from a native CRISPR-Cas system, pACYC-GFP can be used to measure CRISPR interference from non-native Cas effector proteins using *E. coli* as a model system. For this application, Cas effectors and guiding crRNAs are expressed from plasmids. Plasmid-borne CRISPR-Cas systems provide additional flexibility, as a variety of Cas effectors can be tested and plasmids can be easily modified to change the crRNA sequence. Importantly, the pACYCDuet-1 backbone of our reporter plasmid is compatible with several other plasmids, enabling systems in which Cas effector protein(s) and guide RNA can be expressed off multiple plasmids. The use of multiple plasmids may be more necessary for class 1 systems, in which Cas effectors are composed of several protein subunits. For class 2 effectors, the protein and RNA components could either be expressed from the same plasmid or each expressed individually from two different plasmids. Here, we demonstrate the use of our GFP-reporter assay to test the activity of a class 2 Cas effector and guide RNA using a plasmid-based expression system.

4.1 Cas9 fluorescence-based plasmid loss assay

To demonstrate the use of pACYC-GFP with a plasmid-borne Cas effector, we chose the well-characterized Cas9 effector from *Streptococcus pyogenes*. Cas9 requires two RNAs, the guide crRNA and the trans-acting crRNA (tracrRNA), although the two RNAs can be fused into a single-guide RNA (sgRNA) (Jinek et al., 2012). We designed an expression system in which Cas9 is expressed from a plasmid with a pCDF-1b backbone (Cas9-pCDF) and the sgRNA is expressed from pUC19 (sgRNA-pUC19) (Figure 5A). An arabinose inducible promoter (*pBAD*) controls expression of both Cas9 and the sgRNA. Inducible expression allows pACYC-GFP containing a target to be transformed along with the other two plasmids without undergoing interference. Similar to experiments using the native CRISPR-Cas operon, levels of GFP expression can be measured over time after induction and used to show efficiency of targeting by Cas9.

As proof-of-principle, we tested plasmid loss for a perfect target and two mutant targets containing mismatches in the seed region (Figure 5B-C). The targets were inserted into pACYC-GFP between EcoRI and NotI using procedures described in Section 3.1 (Figure 5B). Upon induction of Cas9 and the sgRNA at time point 0, the perfect target was lost steadily over time (Figure 5C). Importantly,

GFP expression did not decrease over the same time course in a culture in which empty pACYC-GFP (lacking a target) was transformed along with Cas9-pCDF and sgRNA-pUC19. This control demonstrates that pACYC-GFP can be stably maintained in the absence of selection even in the presence of two additional plasmids and that plasmid loss only occurs through Cas9-based interference. Interestingly, A PAM-proximal mismatch (G3A) showed no GFP loss while a mismatch further into the seed (G7T) showed GFP loss similar to a perfectly matching target. These results are consistent with previous studies showing that mismatches closer to the PAM are more deleterious for Cas9 targeting (Hsu et al., 2013). Overall, these results demonstrate the utility of the GFP-reporter assay for measuring CRISPR interference from plasmid-borne Cas expression systems. The following sub-sections describe the methods used for measuring pACYC-GFP plasmid loss using the plasmid-borne Cas9/sgRNA-expression system.

4.1.1 Equipment

- Incubator (37°C, for plates and shaking)
- Water bath (42°C)
- Microcentrifuge

4.1.2 Buffer and reagents

- E. coli competent cells
- LB Media
- Carbenicillin (100 mg/mL)
- Chloramphenicol dissolved in 95% ethanol (34 mg/mL)
- Streptomycin (100 mg/mL)
- Arabinose (1M)
- Phosphate Buffered Saline (1X)

4.1.3 Procedure

- 1. Prepare competent cells for desired *E. coli* strain as described in sub-section 3.2.3 (steps 1-5), omitting antibiotic selection in streak plates and cultures. Cells can be aliquoted (50 μL each) into pre-chilled 1.5 mL microcentrifuge tubes, flash frozen in liquid N₂, and stored at -80°C for up to one year. Alternatively, commercially available competent cells can be purchased to ensure high transformation efficiency required for transformation of three plasmids. For the experiment in Figure 5C, we used BL21(DE3) cells.
- 2. To transform, thaw competent cell tubes on ice for 10 minutes. Perform transformation as described in step 7 of section 3.2.3 using 100 ng of Cas9-pCDF, 50 ng of sgRNA-pUC19, and 100 ng pACYC-GFP. For recovery, add 950 μL LB media to each tube and incubate in 37°C shaking incubator for 1 h.
- 3. Spin cells at $2500 \times g$ in microcentrifuge for 5 min. Pour off ~900 μ L of supernatant. Resuspend cells in the remaining ~100 μ L media and plate on LB plates containing 34 μ g/mL chloramphenicol, 100 μ g/mL streptomycin, and 100 μ g/mL carbenicillin. Grow overnight in incubator at 37°C. We generally obtain 20-30 colonies for transformations with three plasmids.
- 4. Create starter cultures by inoculating 2 mL LB media containing 2 μL each of chloramphenicol (34 μg/mL final), streptomycin (100 μg/mL final), and carbenicillin (100 μg/mL final) with a single colony. Grow cultures in a 37°C shaking incubator at 180 rpm overnight or until saturated. We grew three starter cultures for each pACYC-GFP construct as biological replicates.
- 5. Sub-culture 20 μL of starter cultures into 2 mL LB with 2 μL each of streptomycin (100 μg/mL final) and carbenicillin (100 μg/mL final) and induce cells with 20 μL arabinose (20 mM final).
 Continue incubation in a 37°C shaking incubator at 180 rpm. Save the remaining starter culture at 4°C for the first time point (0 h).
- 6. Collect 20 μL samples from each culture starting at 4 h after induction. Samples can be collected at desired intervals and stored at 4°C prior to flow cytometry analysis. For data shown in Figure 5C, we collected samples at 2-3 h intervals, as well as one overnight time point. If an overnight time point is desired, we recommend preparing a fresh culture prior to overnight growth. For the

experiments in Figure 5C, overnight cultures were sub-cultured (1:100 dilution) following 8 h growth.

7. Analyze GFP expression using flow cytometry as described in sub-section 3.3.3 (steps 4-7).

5. SUMMARY AND CONCLUSION

In this chapter, we described a simple method for assessing CRISPR interference in E. coli using a fluorescence-based plasmid loss assay. The assay is based on pACYC-GFP, a carefully designed plasmid that tightly links GFP-based cellular fluorescence to plasmid concentration. CRISPR targets can be easily introduced into pACYC-GFP using a basic restriction cloning strategy. We have also introduced target libraries with randomized PAM or seed sequences to pACYC-GFP to assess the global impact of mutations in these regions on CRISPR-Cas activity (Xue et al., 2015). The efficiency of CRISPR interference against pACYC-GFP can be measured via multiple methods. We demonstrated the use of Typhoon imaging to qualitatively and quantitatively measure the varying levels of pACYC-GFP in E. coli colonies. This method can detect subtle differences in interference that would not manifest in changes in transformation efficiency, as evidenced by the similar number of colonies present on each plate despite the clear variations in plasmid concentration (Figure 3B). We also demonstrated the use of flow cytometry to measure the rate of CRISPR interference for E. coli grown in liquid cultures. This method allows for monitoring interference over time and can reveal less severe defects in plasmid destruction at early time points (e.g. G1C target in Figure 4). Finally, we showed that pACYC-GFP is compatible with a plasmid-borne Cas9/sgRNA expression system. The fluorescence-based CRISPR interference assay is a simple and effective method that could be used to assess the activity of other poorly characterized Cas effectors in *E. coli*.

ACKNOWLEDGEMENTS

The authors would like to thank Karthik Murugan for initial construction of *pBAD*-Cas9 construct, Shawn Rigby of the Iowa State University Flow Cytometry Facility and Joel Nott of the Iowa

State University Protein Facility for help with data collection, and members of the Sashital lab for helpful discussions. This work was supported by grants from the NIH (R01 GM115874) and NSF (1652661).

REFERENCES

- Abudayyeh, O. O., Gootenberg, J. S., Konermann, S., Joung, J., Slaymaker, I. M., Cox, D. B. T., ...

 Zhang, F. (2016). C2c2 is a single-component programmable RNA-guided RNA-targeting CRISPR effector. *Science*, 353(6299). http://doi.org/10.1126/science.aaf5573
- Andersen, J. B., Sternberg, C., Poulsen, L. K., Bjørn, S. P., Givskov, M., & Molin, S. (1998). New Unstable Variants of Green Fluorescent Protein for Studies of Transient Gene Expression in Bacteria. Applied and Environmental Microbiology, 64(6), 2240 LP-2246.
- Brouns, S. J. J., Jore, M. M., Lundgren, M., Westra, E. R., Slijkhuis, R. J. H., Snijders, A. P. L., ... van der Oost, J. (2008). Small CRISPR RNAs guide antiviral defense in prokaryotes. *Science*, 321(5891), 960–4. http://doi.org/10.1126/science.1159689
- Cooper, L. A., Stringer, A. M., & Wade, J. T. (2018). Determining the Specificity of Cascade Binding,

 Interference, and Primed Adaptation In Vivo in the Escherichia coli Type I-E CRISPR-Cas System.

 MBio. http://doi.org/10.1101/169011
- Datsenko, K. A., Pougach, K., Tikhonov, A., Wanner, B. L., Severinov, K., & Semenova, E. (2012).

 Molecular memory of prior infections activates the CRISPR/Cas adaptive bacterial immunity system. *Nature Communications*, *3*, 945. http://doi.org/10.1038/ncomms1937
- De Mey, M., Maertens, J., Lequeux, G. J., Soetaert, W. K., & Vandamme, E. J. (2007). Construction and model-based analysis of a promoter library for E. coli: an indispensable tool for metabolic engineering. *BMC Biotechnology*, 7, 34. http://doi.org/10.1186/1472-6750-7-34
- Deveau, H., Barrangou, R., Garneau, J. E., Labonte, J., Fremaux, C., Boyaval, P., ... Moineau, S. (2008).

 Phage response to CRISPR-encoded resistance in Streptococcus thermophilus. *Journal of Bacteriology*, 190(4), 1390–1400. http://doi.org/10.1128/JB.01412-07
- Elmore, J. R., Sheppard, N. F., Ramia, N., Deighan, T., Li, H., Terns, R. M., & Terns, M. P. (2016).

- Bipartite recognition of target RNAs activates DNA cleavage by the Type III-B CRISPR-Cas system. *Genes & Development*, 30(4), 447–459. http://doi.org/10.1101/gad.272153.115
- Estrella, M. A., Kuo, F.-T., & Bailey, S. (2016). RNA-activated DNA cleavage by the Type III-B CRISPR-Cas effector complex. *Genes & Development*, 30(4), 460–470. http://doi.org/10.1101/gad.273722.115
- Fineran, P. C., Gerritzen, M. J. H., Suárez-Diez, M., Künne, T., Boekhorst, J., van Hijum, S. a F. T., ...

 Brouns, S. J. J. (2014). Degenerate target sites mediate rapid primed CRISPR adaptation.

 Proceedings of the National Academy of Sciences, 111(16), E1629-38.

 http://doi.org/10.1073/pnas.1400071111
- Fu, Y., Foden, J. a, Khayter, C., Maeder, M. L., Reyon, D., Joung, J. K., & Sander, J. D. (2013). High-frequency off-target mutagenesis induced by CRISPR-Cas nucleases in human cells. *Nature Biotechnology*, 31(9), 822–6. http://doi.org/10.1038/nbt.2623
- Garneau, J. E., Dupuis, M. E., Villion, M., Romero, D. A., Barrangou, R., Boyaval, P., ... Moineau, S. (2010). The CRISPR/Cas bacterial immune system cleaves bacteriophage and plasmid DNA.

 Nature, 468(7320), 67–71. http://doi.org/10.1038/nature09523
- Gasiunas, G., Barrangou, R., Horvath, P., & Siksnys, V. (2012). Cas9-crRNA ribonucleoprotein complex mediates specific DNA cleavage for adaptive immunity in bacteria. *Proceedings of the National Academy of Sciences*, 109(39), E2579–E2586. http://doi.org/10.1073/pnas.1208507109
- Hale, C. R., Zhao, P., Olson, S., Duff, M. O., Graveley, B. R., Wells, L., ... Terns, M. P. (2009). RNA-Guided RNA Cleavage by a CRISPR RNA-Cas Protein Complex. *Cell*, 139(5), 945–956. http://doi.org/10.1016/j.cell.2009.07.040
- Hily, J.-M., & Liu, Z. (2009). A simple and sensitive high-throughput GFP screening in woody and herbaceous plants. *Plant Cell Reports*, 28(3), 493–501. http://doi.org/10.1007/s00299-008-0657-z
- Hochstrasser, M. L., Taylor, D. W., Bhat, P., Guegler, C. K., Sternberg, S. H., Nogales, E., & Doudna, J.
 a. (2014). CasA mediates Cas3-catalyzed target degradation during CRISPR RNA-guided interference. *Proceedings of the National Academy of Sciences*, 111(18), 6618–23.

- http://doi.org/10.1073/pnas.1405079111
- Hsu, P. D., Lander, E. S., & Zhang, F. (2014). Development and applications of CRISPR-Cas9 for genome engineering. *Cell*, 157(6), 1262–1278. http://doi.org/10.1016/j.cell.2014.05.010
- Hsu, P. D., Scott, D. a, Weinstein, J. a, Ran, F. A., Konermann, S., Agarwala, V., ... Zhang, F. (2013).
 DNA targeting specificity of RNA-guided Cas9 nucleases. *Nature Biotechnology*, 31(9), 827–32.
 http://doi.org/10.1038/nbt.2647
- Jinek, M., Chylinski, K., Fonfara, I., Hauer, M., Doudna, J. A., & Charpentier, E. (2012). A
 Programmable Dual-RNA-Guided DNA Endonuclease in Adaptive Bacterial Immunity. *Science*,
 337(6096), 816–821. http://doi.org/10.1126/science.1225829
- Jore, M. M., Lundgren, M., van Duijn, E., Bultema, J. B., Westra, E. R., Waghmare, S. P., ... Brouns, S. J. J. (2011). Structural basis for CRISPR RNA-guided DNA recognition by Cascade. *Nature Structural & Molecular Biology*, 18(5), 529–536. http://doi.org/10.1038/nsmb.2019
- Kazlauskiene, M., Tamulaitis, G., Kostiuk, G., Venclovas, Č., & Siksnys, V. (2016). Spatiotemporal Control of Type III-A CRISPR-Cas Immunity: Coupling DNA Degradation with the Target RNA Recognition. *Molecular Cell*, 62(2), 295–306. http://doi.org/10.1016/j.molcel.2016.03.024
- Kim, D., Kim, J., Hur, J. K., Been, K. W., Yoon, S.-H., & Kim, J.-S. (2016). Genome-wide analysis reveals specificities of Cpf1 endonucleases in human cells. *Nature Biotechnology*. http://doi.org/10.1038/nbt.3609
- Kleinstiver, P Benjamin, Pattanayak, Vikram, Prew, M. S., Shengdar, Q. T., Nguyen, T. N., Zheng, Z., & Joung, J. K. (2016). High-fidelity CRISPR-Cas9 nucleases with no detectable genome-wide off-target effects. *Nature*, *529*(7587), 490–495. http://doi.org/10.1038/nature16526
- Koonin, E. V, Makarova, K. S., & Zhang, F. (2017). Diversity, classification and evolution of CRISPR-Cas systems. *Current Opinion in Microbiology*, *37*, 67–78. http://doi.org/10.1016/j.mib.2017.05.008
- Makarova, K. S., Wolf, Y. I., Alkhnbashi, O. S., Costa, F., Shah, S. A., Saunders, S. J., ... Koonin, E. V. (2015). An updated evolutionary classification of CRISPR-Cas systems. *Nature Reviews Microbiology*, 13(11), 722–736. http://doi.org/10.1038/nrmicro3569

- Marraffini, L. A. (2015). CRISPR-Cas immunity in prokaryotes. *Nature*, *526*(7571), 55–61. http://doi.org/10.1038/nature15386
- Medina-Aparicio, L., Rebollar-Flores, J. E., Gallego-Hernández, A. L., Vázquez, A., Olvera, L., Gutiérrez-Ríos, R. M., ... Hernández-Lucas, I. (2011). The CRISPR/Cas immune system is an operon regulated by LeuO, H-NS, and leucine-responsive regulatory protein in Salmonella enterica serovar Typhi. *Journal of Bacteriology*. http://doi.org/10.1128/JB.01480-10
- Mojica, F. J. M., Diez-Villasenor, C., Garcia-Martinez, J., & Almendros, C. (2009). Short motif sequences determine the targets of the prokaryotic CRISPR defence system. *Microbiology*, 155(Pt 3), 733–740. http://doi.org/10.1099/mic.0.023960-0
- Mulepati, S., & Bailey, S. (2013). In vitro reconstitution of an Escherichia coli RNA-guided immune system reveals unidirectional, ATP-dependent degradation of DNA Target. *Journal of Biological Chemistry*, 288(31), 22184–22192. http://doi.org/10.1074/jbc.M113.472233
- Murugan, K., Babu, K., Sundaresan, R., Rajan, R., & Sashital, D. G. D. G. The Revolution Continues:

 Newly Discovered Systems Expand the CRISPR-Cas Toolkit, 68 Molecular Cell 15–25 (2017).

 http://doi.org/10.1016/j.molcel.2017.09.007
- Pougach, K., Semenova, E., Bogdanova, E., Datsenko, K. A., Djordjevic, M., Wanner, B. L., & Severinov, K. (2010). Transcription, processing and function of CRISPR cassettes in Escherichia coli. *Molecular Microbiology*, 77(6), 1367–1379. http://doi.org/10.1111/j.1365-2958.2010.07265.x
- Pul, Ü., Wurm, R., Arslan, Z., Geißen, R., Hofmann, N., & Wagner, R. (2010). Identification and characterization of E. coli CRISPR-cas promoters and their silencing by H-NS. *Molecular Microbiology*, 75(6), 1495–1512. http://doi.org/10.1111/j.1365-2958.2010.07073.x
- Redding, S., Sternberg, S. H., Marshall, M., Gibb, B., Bhat, P., Guegler, C. K., ... Greene, E. C. (2015).

 Surveillance and Processing of Foreign DNA by the Escherichia coli CRISPR-Cas System. *Cell*.

 http://doi.org/10.1016/j.cell.2015.10.003
- Rueden, C. T., Schindelin, J., Hiner, M. C., DeZonia, B. E., Walter, A. E., Arena, E. T., & Eliceiri, K. W. (2017). ImageJ2: ImageJ for the next generation of scientific image data. *BMC Bioinformatics*,

- 18(1), 529. http://doi.org/10.1186/s12859-017-1934-z
- Rutkauskas, M., Sinkunas, T., Songailiene, I., Tikhomirova, M. S., Siksnys, V., & Seidel, R. (2015).

 Directional R-Loop Formation by the CRISPR-Cas Surveillance Complex Cascade Provides

 Efficient Off-Target Site Rejection. *Cell Reports*. http://doi.org/10.1016/j.celrep.2015.01.067
- Sapranauskas, R., Gasiunas, G., Fremaux, C., Barrangou, R., Horvath, P., & Siksnys, V. (2011). The Streptococcus thermophilus CRISPR/Cas system provides immunity in Escherichia coli. *Nucleic Acids Research*, *39*(21), 9275–9282. http://doi.org/10.1093/nar/gkr606
- Sashital, D. G., Wiedenheft, B., & Doudna, J. A. (2012). Mechanism of foreign DNA selection in a bacterial adaptive immune system. *Molecular Cell*, 46(5), 606–615. http://doi.org/10.1016/j.molcel.2012.03.020
- Schneider, C. A., Rasband, W. S., & Eliceiri, K. W. (2012). NIH Image to ImageJ: 25 years of image analysis. *Nature Methods*, 9(7), 671–675.
- Semenova, E., Jore, M. M., Datsenko, K. A., Semenova, A., Westra, E. R., Wanner, B., ... Severinov, K. (2011). Interference by clustered regularly interspaced short palindromic repeat (CRISPR) RNA is governed by a seed sequence. *Proceedings of the National Academy of Sciences*, 108(25), 10098–10103. http://doi.org/10.1073/pnas.1104144108
- Sorek, R., Lawrence, C. M., & Wiedenheft, B. (2013). CRISPR-mediated adaptive immune systems in bacteria and archaea. *Annual Review of Biochemistry*, 82(February), 237–66. http://doi.org/10.1146/annurev-biochem-072911-172315
- Sternberg, S. H., Redding, S., Jinek, M., Greene, E. C., & Doudna, J. A. (2014). DNA interrogation by the CRISPR RNA-guided endonuclease Cas9. *Nature*, 507(7490), 62–7. http://doi.org/10.1038/nature13011
- Swarts, D. C., Makarova, K., Wang, Y., Nakanishi, K., Ketting, R. F., Koonin, E. V, ... van der Oost, J. (2014). The evolutionary journey of Argonaute proteins. *Nature Structural & Molecular Biology*, 21(9), 743–753. http://doi.org/10.1038/nsmb.2879
- Szczelkun, M. D., Tikhomirova, M. S., Sinkunas, T., Gasiunas, G., Karvelis, T., Pschera, P., ... Seidel, R.

- (2014). Direct observation of R-loop formation by single RNA-guided Cas9 and Cascade effector complexes. *Proceedings of the National Academy of Sciences*, 111(27), 9798–803. http://doi.org/10.1073/pnas.1402597111
- van Erp, P. B. G., Jackson, R. N., Carter, J., Golden, S. M., Bailey, S., & Wiedenheft, B. (2015).

 Mechanism of CRISPR-RNA guided recognition of DNA targets in Escherichia coli. *Nucleic Acids Research*. http://doi.org/10.1093/nar/gkv793
- Westra, E. R., Pul, Ü., Heidrich, N., Jore, M. M., Lundgren, M., Stratmann, T., ... Brouns, S. J. J. (2010). H-NS-mediated repression of CRISPR-based immunity in Escherichia coli K12 can be relieved by the transcription activator LeuO. *Molecular Microbiology*, 77(6), 1380–1393. http://doi.org/10.1111/j.1365-2958.2010.07315.x
- Westra, E. R., Semenova, E., Datsenko, K. A., Jackson, R. N., Wiedenheft, B., Severinov, K., & Brouns, S. J. J. (2013). Type I-E CRISPR-Cas Systems Discriminate Target from Non-Target DNA through Base Pairing-Independent PAM Recognition. *PLOS Genetics*, 9(9), e1003742. http://doi.org/10.1371/journal.pgen.1003742
- Westra, E. R., van Erp, P. B. G., Künne, T., Wong, S. P., Staals, R. H. J., Seegers, C. L. C., ... van der Oost, J. (2012). CRISPR Immunity Relies on the Consecutive Binding and Degradation of Negatively Supercoiled Invader DNA by Cascade and Cas3. *Molecular Cell*, 46(5), 595–605. http://doi.org/10.1016/j.molcel.2012.03.018
- Wiedenheft, B., van Duijn, E., Bultema, J., Waghmare, S., Zhou, K., Barendregt, A., ... Doudna, J. A. (2011). RNA-guided complex from a bacterial immune system enhances target recognition through seed sequence interactions. *Proceedings of the National Academy of Sciences*. http://doi.org/10.1073/pnas.1102716108
- Xue, C., Seetharam, A. S., Musharova, O., Severinov, K., J Brouns, S. J., Severin, A. J., & Sashital, D. G. (2015). CRISPR interference and priming varies with individual spacer sequences. *Nucleic Acids Research*, 43(22), 10831–47. http://doi.org/10.1093/nar/gkv1259
- Xue, C., Whitis, N. R., & Sashital, D. G. (2016). Conformational Control of Cascade Interference and

- Priming Activities in CRISPR Immunity. *Molecular Cell*, *64*(4), 826–834. http://doi.org/10.1016/j.molcel.2016.09.033
- Xue, C., Zhu, Y., Zhang, X., Shin, Y.-K., & Sashital, D. G. (2017). Real-Time Observation of Target Search by the CRISPR Surveillance Complex Cascade. *Cell Reports*, 21(13). http://doi.org/10.1016/j.celrep.2017.11.110
- Zetsche, B., Gootenberg, J. S., Abudayyeh, O. O., Slaymaker, I. M., Makarova, K. S., Essletzbichler, P., ... Zhang, F. (2015). Cpf1 Is a Single RNA-Guided Endonuclease of a Class 2 CRISPR-Cas System. *Cell*, 163(3), 759–771. http://doi.org/10.1016/j.cell.2015.09.038

FIGURE LEGENDS

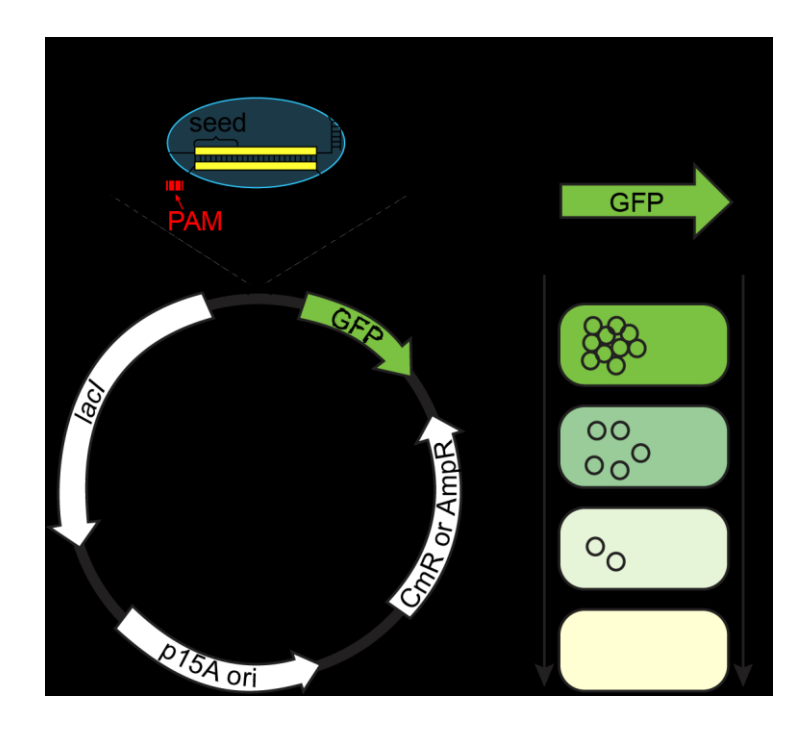


Figure 1: Design of fluorescence-based CRISPR interference assay. A. Schematic of Cas-crRNA effector complex bound to dsDNA. The spacer-protospacer RNA:DNA hybrid is shown in yellow. The PAM is highlighted in red. The PAM-proximal seed region is labeled. B. Schematic of pACYC-GFP plasmid. MCS1: multiple cloning site 1. C. Close-up schematic of GFP expression cassette in pACYC-GFP. The locations of the constitutive promoter and *ssrA* degradation tag are highlighted. D. Basis for fluorescence-based plasmid loss assay. As the plasmid concentration decreases due to CRISPR-based plasmid loss, the cells become less fluorescent.

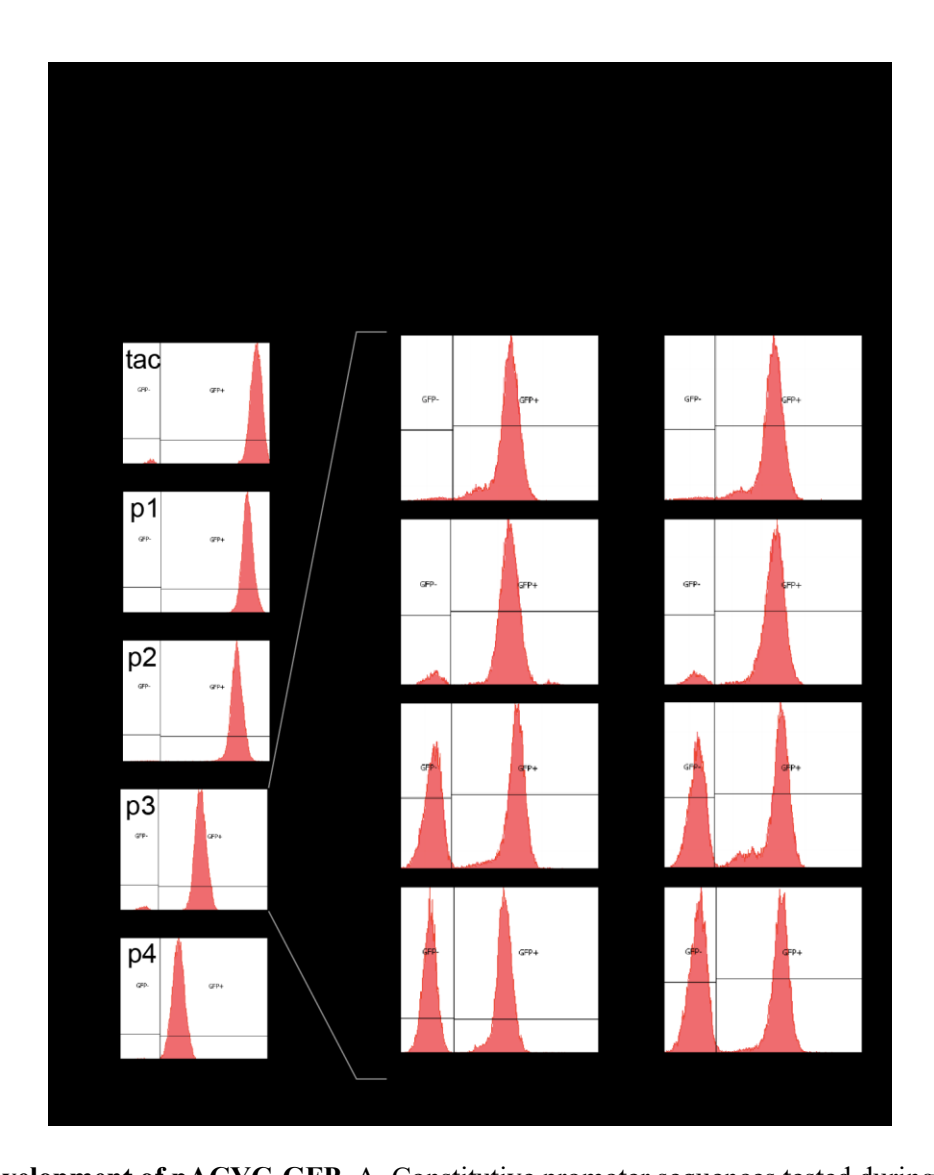


Figure 2: Development of pACYC-GFP. A. Constitutive promoter sequences tested during construction of pACYC-GFP. Promoters 1-4 are variants of *tac* promoter that reduce the promoter strength. Promoter 1 contains an extra base pair between the -10 and -35 sites. Promoters 2, 3 and 4 contain one, two or three variations in the -35 site, respectively. Variations between promoters are underlined. Gaps in aligned promoter sequences are represented with spaces. B. Flow cytometry histograms for the five promoters tested. p1-p4: promoters 1-4. C. Competition assays between cells harboring pACYCDuet-1 (GFP-) and pACYC-GFP (GFP+). The population distribution remains the same after 24 h of growth, indicating that pACYC-GFP does not affect growth rate of the cells.

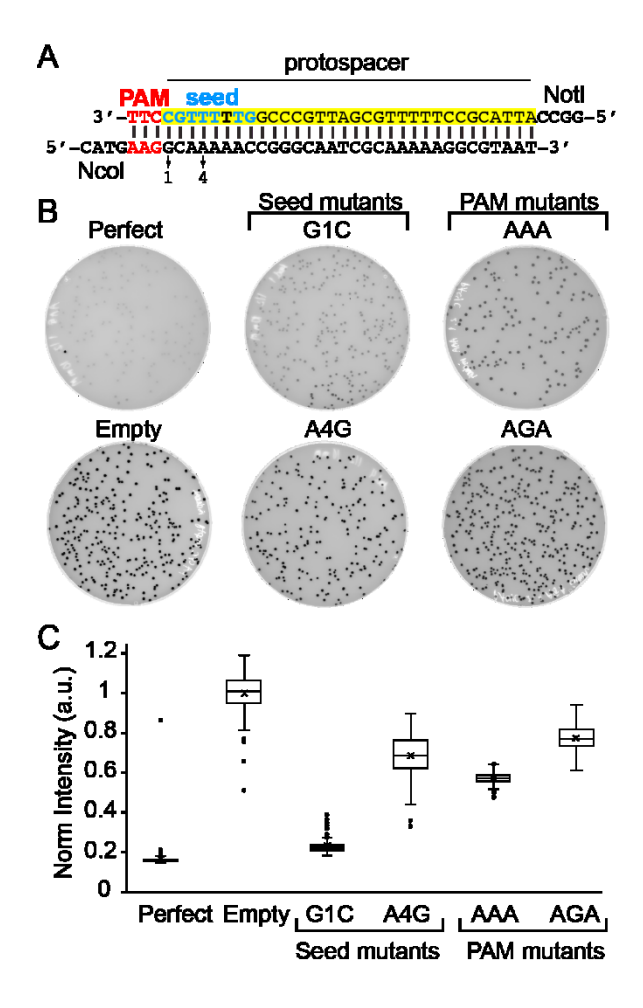


Figure 3: Detecting CRISPR interference in bacterial colonies. A. Design of target sequence inserted into pACYC-GFP. The perfect target is shown, similar oligonucleotides bearing G1C, A4G, AAA PAM or AGA PAM (non-target strand sequences) mutations were used for mutant target sequences. Positions of seed mutations are indicated. The target-strand protospacer is highlighted in yellow, the seed in blue, and the PAM in red. NcoI and NotI overhangs are labeled. B. Typhoon scanned plates for perfect target, empty pACYC-GFP lacking a CRISPR target, and the four mutant target plasmids. C. Box plot of quantified intensities for colonies on each plate. The mean intensity for each colony was normalized against the average mean intensity for colonies from the empty pACYC-GFP plate ([mean intensity induced colony]/[average mean intensity for all empty pACYC-GFP colonies]). Boxes depict variation from 25th to 75th percentile with the line within the box representing the median value and the X marking the mean. Error bars depict the local minimum and maximum, outliers are shown as circles.

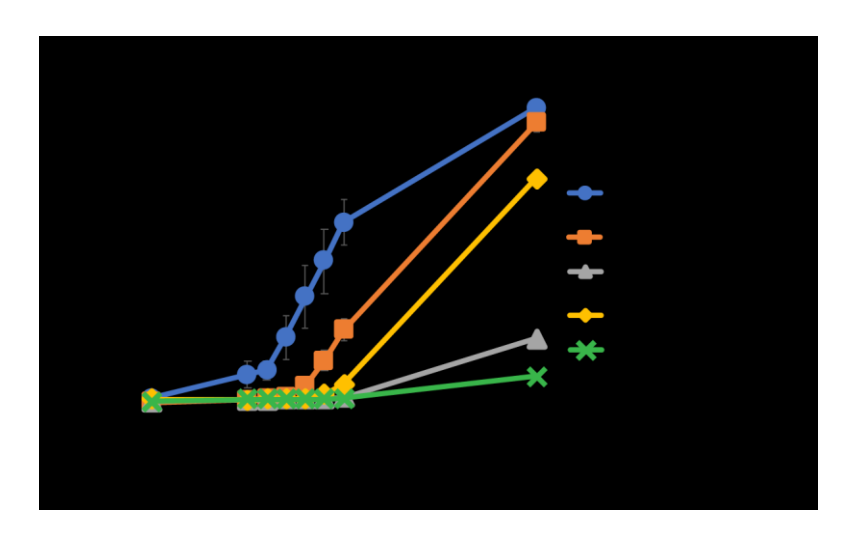


Figure 4: Monitoring CRISPR interference over time in liquid cultures. Plasmid loss (%) is the percentage of GFP- cells based on flow cytometry measurements at each time point. The average plasmid loss from 2-4 replicates is shown, with error representing standard deviation.

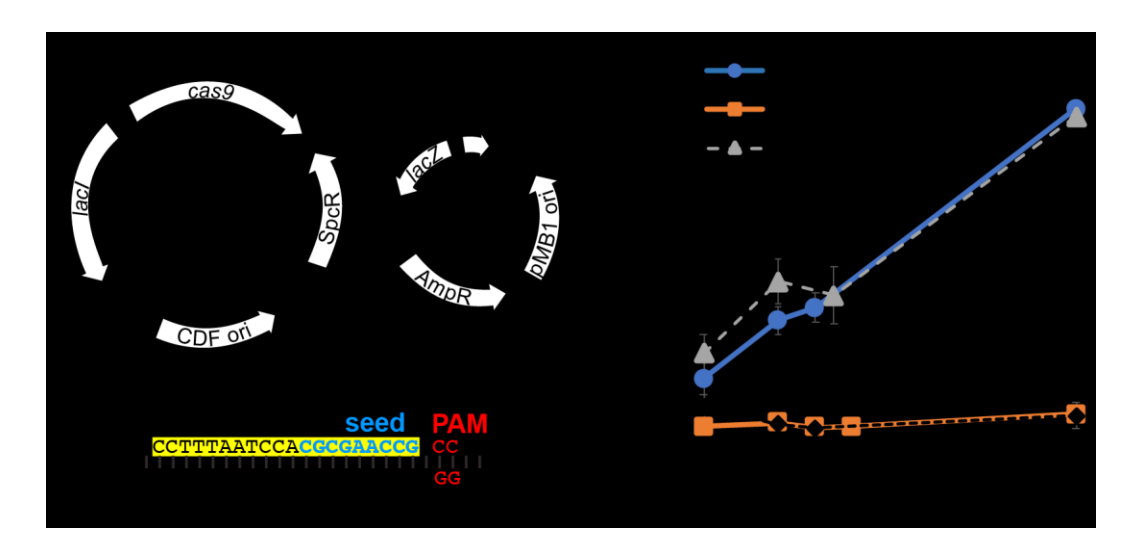


Figure 5: Measurement of Cas9 cleavage using GFP reporter assay. A. Schematic of *cas9* and gRNA expression plasmids. The *cas9* gene and sgRNA are both expressed from arabinose inducible *pBAD* promoters. B. Target inserted into pACYC-GFP for this study. The target-strand protospacer is highlighted in yellow, the seed in blue, and the PAM in red. EcoRI and NotI overhangs are labeled. Positions of G3A or G7T (non-target strand sequence) mutations are indicated. C. Plasmid loss assay for Cas9 targets containing a perfect sequence or seed mismatches at the third or seventh position. Empty pACYC-GFP (no target) was used as a control to ensure that the plasmid is stable in the absence of CRISPR interference. Plasmid loss (%) is the percentage of GFP- cells based on flow cytometry measurements at each time point. The average plasmid loss from 3 replicates is shown, with error representing standard deviation.